Acta Crystallographica Section A
Foundations of Crystallography
ISSN 0108-7673

Received 13 February 2013
Accepted 4 August 2013

Distribution rules of systematic absences on the Conway topograph and their application to powder auto-indexing

R. Oishi-Tomiyasu

High Energy Accelerator Research Organization, Tsukuba, Ibaraki, Japan. Correspondence e-mail: ryoko.tomiyasu@kek.jp

This paper presents several general properties of systematic absences that are available before unit-cell parameters and the space group have been determined. The properties are given in the form of distribution rules of Miller indices corresponding to systematic absences on a *topograph*. A topograph is a graph whose edges are associated with a set of four lattice vectors satisfying Ito's equation $2(|l_1^*|^2 + |l_2^*|^2) = |l_1^* + l_2^*|^2 + |l_1^* - l_2^*|^2$. It is possible to integrate global information about extinct reflections by using topographs. As an example of the application of these rules, a new powder auto-indexing algorithm is introduced, focusing on its theoretical aspects.

1. Introduction

When Γ_{ext} is the set of Miller indices that are extinct due to systematic absences, it is impossible to extract the lengths of lattice vectors l^* belonging to Γ_{ext} from powder diffraction patterns. Because of this, some powder auto-indexing programs have tables of systematic absences in order to reduce their adverse effects. However, it is not straightforward to use such tables without complicating and slowing the algorithm before the unit-cell parameters have been determined. The aim of this study is to provide new types of common properties of systematic absences that are available before the unit-cell parameters are determined. Although we focus on powder auto-indexing in this paper, our approach would also be effective in any kind of unit-cell parameter determination.

A *topograph* is a graph whose edges are associated with a set of lattice vectors l_1, l_2, $l_1 \pm l_2$, as in Fig. 1 of §3. These vectors satisfy Ito's equation $2(|l_1|^2 + |l_2|^2) = |l_1 + l_2|^2 + |l_1 - l_2|^2$ used in Ito's method (Ito, 1949). In §3, we explain the basic properties of topographs defined for two- and three-dimensional lattices. Using topographs, we can analyse the relationship between the two sets of lattice vectors $\{l_1, l_2, l_1 \pm l_2\}$ and $\{k_1, k_2, k_1 \pm k_2\}$.

In §4, we present a common property of the systematic absences of wallpaper groups (Theorem 1) so as to facilitate understanding of the case of space groups. The property is described by the distribution rules of elements of Γ_{ext} on a *topograph*, which were originally defined in the reduction theory of positive-definite quadratic forms (Conway, 1997). From this property, Ito's method (Ito, 1949; de Wolff, 1958) is effective for unit-cell parameter determination of two-dimensional lattices, regardless of the systematic absences of wallpaper groups. However, this is not the case for space groups. In Appendix *A* of the supplementary material,[1] we present types of systematic absences for which Ito's method is considered to fail, or at least encounter a difficult situation.

Nevertheless, systematic absences of space groups are proved to have similar properties to those of wallpaper groups (Theorems 2–4). By using the following equation instead of Ito's equation, an algorithm which is effective for all types of systematic absences is gained:

$$3|l_1|^2 + |l_1 + 2l_2|^2 = 3|l_2|^2 + |2l_1 + l_2|^2. \quad (1)$$

In §5, we introduce the mathematical results in parallel with an explanation of the new powder auto-indexing algorithm. Although the new auto-indexing method also utilizes Ito's equation, the remaining parts are largely different from de Wolff's method adopted in Visser's program (Visser, 1969). Error-stable Bravais-lattice determination is required afterwards in order to complete powder auto-indexing. We have already contributed to reducing the time for error-stable Bravais-lattice determination in Oishi-Tomiyasu (2012).

As another application of topographs, we define a new sorting criterion for zones. This criterion is used in our powder auto-indexing algorithm for zone detection in order to reduce the computational time considerably.

The content of this paper focuses on the theoretical aspects of the new algorithm. Technical issues, including parameter settings, results and other advantages such as computational speed and robustness against missing or false peaks, will be explained in our subsequent paper on the new powder auto-indexing software *Conograph*.

[1] Appendices *A*, *B*, *C* and *D* of this paper are available from the IUCr electronic archives (Reference: SC5063). Services for accessing them are described at the back of the journal.

Notation and symbols. We summarize the notation and symbols used throughout the paper. The inner product of the Euclidean space $\mathbb{R}^N$ is denoted by $u \cdot v$ and the Euclidean norm $u \cdot u$ is denoted by $|u|^2$. Any basis $v_1, \ldots, v_N$ of an N-dimensional lattice L is associated with an $N \times N$ symmetric matrix $(v_i \cdot v_j)_{1 \le i,j \le N}$, which is called a *metric tensor* of L.

If a set $\{v_1, \ldots, v_i\} \subset L$ $(1 \le i < N)$ is extended to a basis $v_1, \ldots, v_N$ of L, the set is called *a primitive set* of L. In particular, v is called a *primitive vector* of L if and only if $\{v\}$ is a primitive set of L.

For a crystal, its *primitive lattice* is the lattice consisting of all the translations that preserve the crystal structure. Wallpaper groups and space groups are collectively called crystallographic groups when the dimension of the lattice is not fixed.

2. Types of systematic absence

Any crystallographic group G is represented as the semidirect $R_G \ltimes L$, where R_G is a point group of G and L is the lattice consisting of all the translations in G. All the *types* of systematic absence are determined by the following two factors: (*a*) the isomorphism class of G, (*b*) the conjugacy class of the site symmetry group H in G. [More precisely, the subgroup $R_H \subset R_G$ corresponding to H and the set of Wyckoff positions are used to represent H in *International Tables for Crystallography* (Hahn, 1983).]

There are only finitely many types of systematic absence when the dimension of the lattice L is fixed. Furthermore, for $N = 2, 3$, the following fact is ascertained from the list of systematic absences in *International Tables for Crystallography* (although this is true for general N, the general case is not necessary here).

Fact 1. Let M be the order of the point group R_G of G and L^* be the reciprocal lattice of L. If $\Gamma_{\rm ext} \subset L^*$ is the subset corresponding to the systematic absences of the type determined by G and H, there exist $\mathcal{H} \subset \mathbb{R}^N$, a union of finite linear subspaces of dimension less than N and a subset $\Omega \subset L^*/ML^*$ such that the following holds for any $l^* \in L^*$ not contained in $\mathcal{H}$:

$$l^* \in \Gamma_{\rm ext} \Longleftrightarrow l^* + ML^* \in \Omega. \tag{2}$$

For instance, the order of R_G of the space group $P4_232$ (No. 208) equals 24. For the space group, the type with the Wyckoff letter i, j has

$$\begin{aligned}\Gamma_{\rm ext} = \{[hkl] : h, k, l \text{ are odd and distinct}\} \cup \{[hhl] : l \text{ is odd}\} \\ \cup \{[hkh] : k \text{ is odd}\} \cup \{[hkk] : h \text{ is odd}\}.\end{aligned} \tag{3}$$

If the two-dimensional planes in the reciprocal space including all of $[hhl]$, $[hkh]$, $[hkk]$ are denoted by $\mathcal{H}_{[hhl]}$, $\mathcal{H}_{[hkh]}$, $\mathcal{H}_{[hkk]}$, respectively, $\mathcal{H}$ and Ω in Fact 1 can be chosen as follows:

$$\mathcal{H} = \mathcal{H}_{[hhl]} \cup \mathcal{H}_{[hkh]} \cup \mathcal{H}_{[hkk]}, \tag{4}$$

$$\Omega = \{[hkl] \in L^*/24L^* : h, k, l \text{ are odd}\}. \tag{5}$$

Fact 1 was used to prove the theorems in §5.

3. Topographs for low-dimensional lattices

Topographs were originally introduced in Conway (1997) as a picturesque method to explain the Selling reduction (Selling, 1874) of 2×2 metric tensors [the Selling reduction is also called the Delaunay reduction in crystallography (Delaunay, 1933)]. An application of topographs to powder auto-indexing was proposed first in Oishi-Tomiyasu *et al.* (2009).

In the following sections, the structures of topographs for two-dimensional and three-dimensional lattices are explained. We refer to Conway (1997) for a more detailed explanation of two-dimensional cases. We shall omit the case of higher-dimensional lattices for simplicity, although the definition of topographs is generalized to any-dimensional lattices by using C-type domains (Ryshkov, 1976), retaining the association of topograph edges with lattice vectors satisfying Ito's equation. The relation between C-type domains and Ito's equation seems not to have been mentioned in the literature.

3.1. Topographs for two-dimensional lattices

For any fixed two-dimensional lattice L, the set of all nodes of the *topograph* is identified with the following V_2:

$$V_2 := \big\{\{0, \pm l_1, \pm l_2, \pm(l_1 + l_2)\} : \langle l_1, l_2\rangle \text{ is a basis of } L\big\}. \tag{6}$$

Every $\Phi \in V_2$ consists of seven vectors, including 0. We denote the node corresponding to $\Phi \in V_2$ by $v(\Phi)$. In the topograph, two nodes $v(\Phi_1)$, $v(\Phi_2)$ are connected by an edge if and only if the number of elements in $\Phi_1 \cap \Phi_2$ equals 5. This holds if and only if there exist $0 \neq k_1, k_2 \in L$ such that $\Phi_1 = (\Phi_1 \cap \Phi_2) \cup \{\pm k_1\}$ and $\Phi_2 = (\Phi_1 \cap \Phi_2) \cup \{\pm k_2\}$. It is straightforward to check that both $(k_1 \pm k_2)/2$ are contained in $\Phi_1 \cap \Phi_2$ in this case, and $\langle (k_1 + k_2)/2, (k_1 - k_2)/2\rangle$ is a basis of L.

As a result, the edge connecting $v(\Phi_1)$ and $v(\Phi_2)$ may be considered to be associated with the following Ito's equation:

$$2\left(\left|\frac{k_1 + k_2}{2}\right|^2 + \left|\frac{k_1 - k_2}{2}\right|^2\right) = |k_1|^2 + |k_2|^2. \tag{7}$$

From the lengths in equation (7), as in Ito's method, a 2×2 metric tensor of L is retrieved by

$$\begin{pmatrix} \left|\frac{k_1+k_2}{2}\right|^2 & \frac{|k_i|^2 - \left|\frac{k_1+k_2}{2}\right|^2 - \left|\frac{k_1-k_2}{2}\right|^2}{2} \\ \frac{|k_i|^2 - \left|\frac{k_1+k_2}{2}\right|^2 - \left|\frac{k_1-k_2}{2}\right|^2}{2} & \left|\frac{k_1-k_2}{2}\right|^2 \end{pmatrix} (i = 1, 2). \tag{8}$$

It does not matter whether $i = 1$ or 2 is used in equation (8), because the 2×2 metric tensors obtained are equal within a change of basis as seen from the following equation:

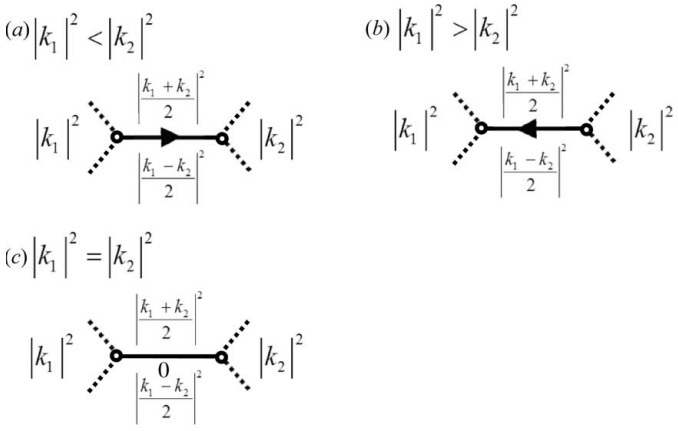

Figure 1
Edges of a topograph for a two-dimensional lattice. [Here, we assume the left and right nodes correspond to $\Phi_1 := \{0, \pm(k_1 \pm k_2)/2, \pm k_1\}$ and $\Phi_2 := \{0, \pm(k_1 \pm k_2)/2, \pm k_2\}$, respectively. The direction of every edge of a topograph is determined using the lengths of k_1 and k_2.]

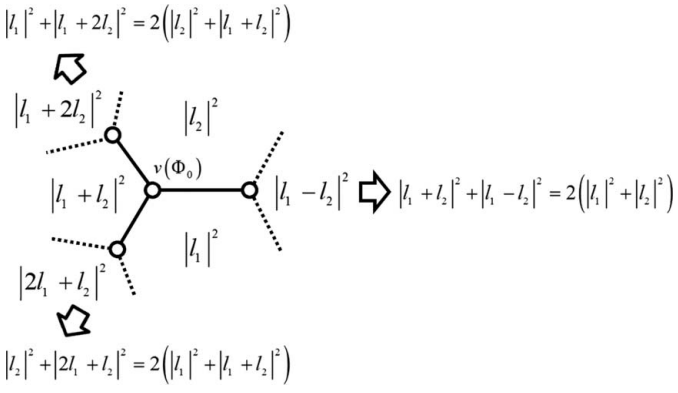

Figure 2
Local structure of a topograph defined for a two-dimensional lattice. [For a fixed basis $\langle l_1, l_2\rangle$ of L, define $\Phi_0 := \{0, \pm l_1, \pm l_2, \pm(l_1 + l_2)\}$. Then, the node $v(\Phi_0)$ is an endpoint of the three edges above.]

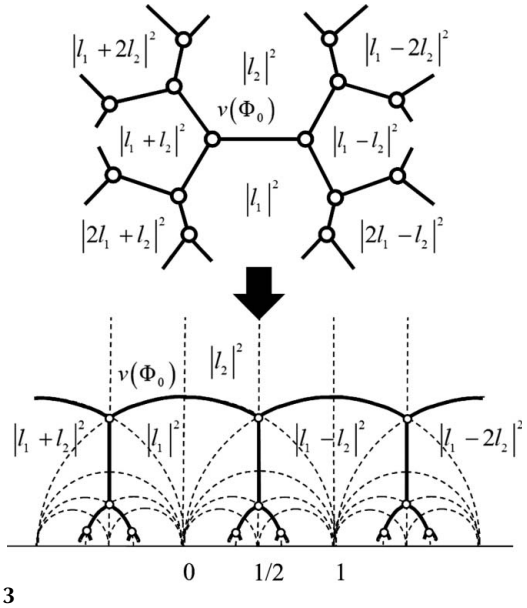

Figure 3
Embedding of a topograph in the upper half plane.

$$\begin{pmatrix} |\frac{k_1+k_2}{2}|^2 & \frac{|k_1|^2-|\frac{k_1+k_2}{2}|^2-|\frac{k_1-k_2}{2}|^2}{2} \\ \frac{|k_1|^2-|\frac{k_1+k_2}{2}|^2-|\frac{k_1-k_2}{2}|^2}{2} & |\frac{k_1-k_2}{2}|^2 \end{pmatrix} = \begin{pmatrix} 1 & 0 \\ 0 & -1 \end{pmatrix} \begin{pmatrix} |\frac{k_1+k_2}{2}|^2 & \frac{|k_2|^2-|\frac{k_1+k_2}{2}|^2-|\frac{k_1-k_2}{2}|^2}{2} \\ \frac{|k_2|^2-|\frac{k_1+k_2}{2}|^2-|\frac{k_1-k_2}{2}|^2}{2} & |\frac{k_1-k_2}{2}|^2 \end{pmatrix} \begin{pmatrix} 1 & 0 \\ 0 & -1 \end{pmatrix}. \quad (9)$$

In a topograph, the direction of every edge is determined as in Fig. 1. (The edge directions are omitted in the following discussion if unnecessary.) Every node is an endpoint of three edges, as in Fig. 2. In general, different edges of the same topograph provide 2×2 metric tensors of L with regard to difference bases. For example, this holds for the three Ito equations in Fig. 2 as follows:

$$\begin{aligned} &\begin{pmatrix} |l_1|^2 & \frac{|l_1+l_2|^2-|l_1|^2-|l_2|^2}{2} \\ \frac{|l_1+l_2|^2-|l_1|^2-|l_2|^2}{2} & |l_2|^2 \end{pmatrix} \\ &= \begin{pmatrix} 1 & 1 \\ 0 & -1 \end{pmatrix} \begin{pmatrix} |l_1+l_2|^2 & \frac{|l_1|^2-|l_2|^2-|l_1+l_2|^2}{2} \\ \frac{|l_1|^2-|l_2|^2-|l_1+l_2|^2}{2} & |l_2|^2 \end{pmatrix} \begin{pmatrix} 1 & 0 \\ 1 & -1 \end{pmatrix} \\ &= \begin{pmatrix} -1 & 0 \\ 1 & 1 \end{pmatrix} \begin{pmatrix} |l_1|^2 & \frac{|l_2|^2-|l_1|^2-|l_1+l_2|^2}{2} \\ \frac{|l_2|^2-|l_1|^2-|l_1+l_2|^2}{2} & |l_1+l_2|^2 \end{pmatrix} \begin{pmatrix} -1 & 1 \\ 0 & 1 \end{pmatrix}. \end{aligned} \quad (10)$$

Regardless of the selected L, topographs for two-dimensional lattices have the same graph structure and are embedded in the upper hyperplane, as in Fig. 3. It has been proved that they are connected trees, *i.e.* there exists a unique path between any two nodes $v(\Phi_1)$ and $v(\Phi_2)$ (*cf.* ch. 1, Conway, 1997).

3.2. Topographs for three-dimensional lattices

For any fixed three-dimensional lattice L, the topograph has the following V_3 as the set of all nodes:

$$V_3 := \left\{ \begin{Bmatrix} 0, \pm l_1, \pm l_2, \pm l_3, \\ \pm(l_1 + l_2 + l_3), \\ \pm(l_1 + l_2), \pm(l_1 + l_3), \\ \pm(l_2 + l_3) \end{Bmatrix} : \langle l_1, l_2, l_3\rangle \text{ is a basis of } L \right\}. \quad (11)$$

Every $\Phi \in V_3$ consists of 15 elements, including 0. Two nodes $v(\Phi_1), v(\Phi_2)$ are connected by an edge if and only if the number of elements in $|\Phi_1 \cap \Phi_2|$ equals 13. In this case, the following holds.

Lemma 1. For any fixed basis $\langle l_1, l_2, l_3\rangle$ of L, we define $l_4 := -l_1 - l_2 - l_3$ and $\Phi_1 := \{0, \pm l_1, \pm l_2, \pm l_3, \pm l_4, \pm(l_1 + l_2), \pm(l_1 + l_3), \pm(l_2 + l_3)\}$. If $\Phi_1, \Phi_2 \in V_3$ satisfy $|\Phi_1 \cap \Phi_2| = 13$, $\Phi_1 = (\Phi_1 \cap \Phi_2) \cup \{\pm(l_i + l_j)\}$ and $\Phi_2 = (\Phi_1 \cap \Phi_2) \cup \{\pm(l_i - l_j)\}$ hold for some $1 \le i < j \le 4$.

A proof of Lemma 1 is provided in Appendix *B*. As a result of Lemma 1, if $k_1, k_2 \in L$ are chosen so that $\Phi_1 = (\Phi_1 \cap \Phi_2) \cup \{\pm k_1\}$ and $\Phi_2 = (\Phi_1 \cap \Phi_2) \cup \{\pm k_2\}$, $\{(k_1 + k_2)/2, (k_1 - k_2)/2\}$ is a primitive set of L, and both $(k_1 \pm k_2)/2$ are contained in $\Phi_1 \cap \Phi_2$. Hence the edge

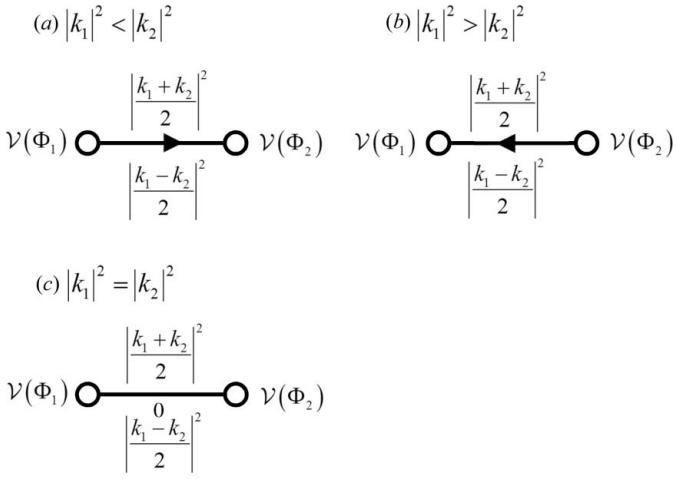

Figure 4
Edges of a topograph for a three-dimensional lattice. [Here, we assume $\Phi_1 = (\Phi_1 \cap \Phi_2) \cup \{\pm k_1\}$ and $\Phi_2 = (\Phi_1 \cap \Phi_2) \cup \{\pm k_2\}$. Differently from Fig. 1, $|k_1|^2$, $|k_2|^2$ are omitted.]

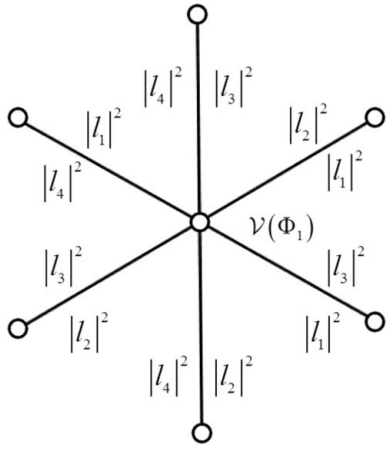

Figure 5
Local structure of a topograph defined for a three-dimensional lattice. For any fixed basis $\langle l_1, l_2, l_3\rangle$ of L, choose l_4 and Φ_1 as in Lemma 1. The node $v(\Phi_1)$ is an endpoint of the six edges associated with the set of vectors l_i, l_j, $l_i \pm l_j$ $(1 \le i < j \le 4)$.

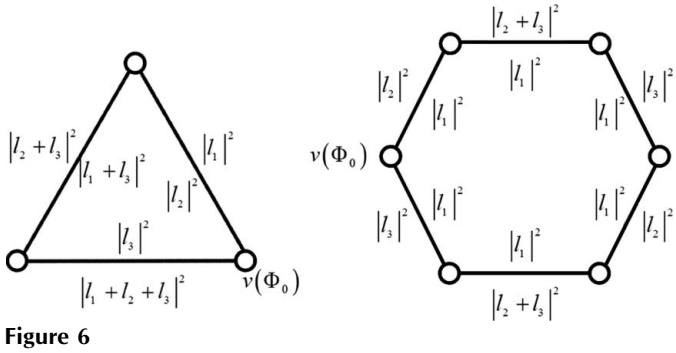

Figure 6
Circuits contained in the topograph for a three-dimensional lattice L. [For any fixed basis $\langle l_1, l_2, l_3\rangle$ of L, we define $\Phi_0 := \{0, \pm l_1, \pm l_2, \pm l_3, \pm(l_1+l_2), \pm(l_1+l_3), \pm(l_2+l_3), \pm(l_1+l_2+l_3)\}$. In Appendix C, it is proved that these circuits generate the fundamental group of the topograph.]

connecting $v(\Phi_1)$ and $v(\Phi_2)$ may be considered to be associated with the Ito equation in equation (7), similarly with the two-dimensional case.

In the three-dimensional case, every edge is tentatively represented as in Fig. 4. By Lemma 1, every topograph node is an endpoint of six edges as in Fig. 5.

Topographs for three-dimensional lattices are connected, *i.e.* paths exist between any two nodes although they are not a tree (see Corollary C.1 in Appendix *C*). The simple circuits of length less than 7 in the topographs are listed in Fig. 6. (A path containing no repeated vertices or edges other than the starting and ending vertices is called a *simple circuit*.)

In §5, information about the lengths associated with the circuits of length 6 are used to generate candidate powder auto-indexing solutions.

4. Distribution rules for wallpaper groups

This section aims to introduce distribution rules for wallpaper groups and provide some information about the framework of the new algorithm. When $\Gamma_{\rm ext}$ is the set of reciprocal-lattice vectors corresponding to extinct reflections due to the systematic absence, Theorem 1 claims that elements of $\Gamma_{\rm ext}$ only appear in the grey area in Fig. 7, regardless of the type of systematic absence.

Theorem 1. We fix a type of systematic absence belonging to a wallpaper group G, and let L be the set of all translations in G and L^* be the reciprocal lattice of L. If l^* is a primitive vector of L^* belonging to $\Gamma_{\rm ext}$, L^* has a basis $\langle l_1^*, l_2^*\rangle$ satisfying $l_1^* \cdot l_2^* = 0$. Furthermore, l^* equals $\pm l_1^*$ or $\pm l_2^*$.

Theorem 1 is easily verified by checking the systematic absences of wallpaper groups in *International Tables for Crystallography*. When Theorem 1 is considered from the point of view of powder auto-indexing, the following results are obtained:

(*P*1) Ito's method works appropriately, for any types of systematic absence of wallpaper groups, because L^* has infinitely many basis vectors $\langle l_1^*, l_2^*\rangle$ such that none of l_1^*, l_2^*, $l_1^* \pm l_2^*$ belongs to $\Gamma_{\rm ext}$.

(*P*2) Furthermore, the topograph contains connected subgraphs consisting of infinitely many edges associated with l_1^*, l_2^*, $l_1^* \pm l_2^* \notin \Gamma_{\rm ext}$.

The former property (*P*1) indicates that the array *Ans* output by the algorithm in Table 1 contains the 2×2 metric

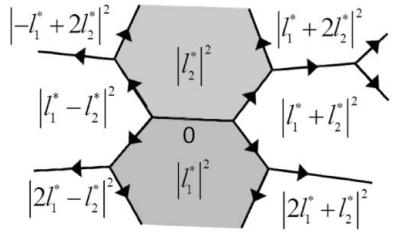

Figure 7
Reciprocal-lattice vectors allowed to correspond to systematic absences. [Any topographs include (if any) a unique edge with the direction 0. This is proved in ch. 1 of Conway (1997) as the case of a *double well*.]

Table 1
Algorithm to search for four q-values satisfying Ito's equation.

void enumerateItoSolutions(Λ^{obs}, c, Ans)

(Input) Λ^{obs} : array of q-values* $q_1, \ldots, q_{N_{peak}}$ of diffraction peaks. We assume that the approximate errors $\mathrm{Err}(q_i + q_j)$ of $q_i + q_j$ are available.
$c > 0$: error tolerance level
(Output) Ans : array of 2×2 metric tensors†

Sort a sequence $S := \langle q_i + q_j : 1 \le i \le j \le N_{peak} \rangle$ in ascending order.
for $i := 1$ to $\frac{1}{2}N_{peak}(N_{peak}+1)$ do
  Suppose $S[i] = q_r + q_s$.
  Take integers $1 \le J_{min}, J_{max} \le N_{peak}$ satisfying
  $J_{min} \le j \le J_{max} \iff |2S[i] - S[j]| \le 2c\mathrm{Err}(q_r + q_s)$.
  for $j := J_{min}$ to J_{max} do
    Suppose $S[j] = q_t + q_u$.
    if $|2(q_r + q_s) - q_t - q_u| \le c\mathrm{Err}(q_t + q_u)$ then
      $S := \begin{pmatrix} q_r & \frac{q_t - q_r - q_s}{2} \\ \frac{q_t - q_r - q_s}{2} & q_s \end{pmatrix}$.
      if $\det S > 0$ then
        insert S in Ans.
      end if
    end if
  end for
end for

† The unit-cell parameters are retrieved from the metric tensor of L^* by carrying out Bravais-lattice determination.

tensor of the true solution, when the q-values of diffraction peaks are extracted appropriately.

The latter property ($P2$) allows us to define a new sorting criterion for two-dimensional lattices using topographs. This enables us to judge which 2×2 metric tensors output from Table 1 are more plausible solutions. In order to explain this, we shall start from the upper subgraph in Fig. 8, making the same assumption as used in Ito's method.

Assumption. For q-values q_1, q_2, q_3, q_4 extracted from diffraction patterns satisfying $2(q_1 + q_2) = q_3 + q_4$, there exist lattice vectors l_1^*, l_2^* of L^* such that $q_1 = |l_1^*|^2$, $q_2 = |l_2^*|^2$, $q_3 = |l_1^* + l_2^*|^2$, $q_4 = |l_1^* - l_2^*|^2$ holds.

If the above assumption is true, and if missing reflections owing to systematic absences or other reasons can be neglected, all $|2l_1^* \pm l_2^*|^2$ and $|l_1^* \pm 2l_2^*|^2$ in the following equations will also be observed as q-values of diffraction peaks:

$$2(|l_1^*|^2 + |l_1^* + l_2^*|^2) = |l_2^*|^2 + |2l_1^* + l_2^*|^2, \quad (12)$$

$$2(|l_2^*|^2 + |l_1^* + l_2^*|^2) = |l_1^*|^2 + |l_1^* + 2l_2^*|^2, \quad (13)$$

$$2(|l_1^*|^2 + |l_1^* - l_2^*|^2) = |l_2^*|^2 + |2l_1^* - l_2^*|^2, \quad (14)$$

$$2(|l_2^*|^2 + |l_1^* - l_2^*|^2) = |l_1^*|^2 + |l_1^* - 2l_2^*|^2. \quad (15)$$

On the other hand, if there are no l_1^*, l_2^* satisfying the assumption [because either q_1, q_2, q_3 or q_4 corresponds to a false peak caused by impurities in a material, or $2(q_1 + q_2) = q_3 + q_4$ holds accidentally], it is very rare that one of $|2l_1^* \pm l_2^*|^2$, $|l_1^* \pm 2l_2^*|^2$ will 'accidentally' be observed again.

Therefore, we shall extend the graph in Fig. 8 by unifying each edge, as long as all the four lattice vector lengths in its

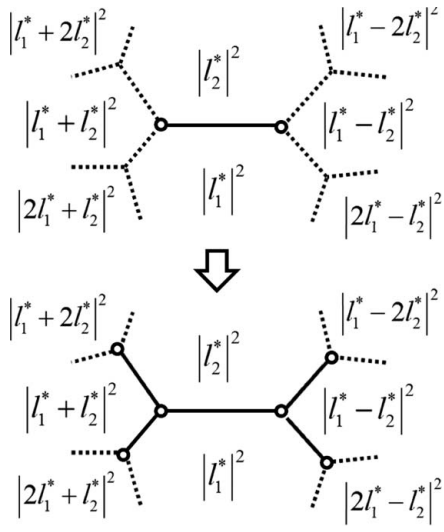

Figure 8
A subgraph corresponding to the formula $2(|l_1^*|^2 + |l_2^*|^2) = |l_1^* + l_2^*|^2 + |l_1^* - l_2^*|^2$ and its extension using equations (12)–(15).

corresponding Ito equation are observed as q-values of diffraction peaks. The resulting graph would then become much larger if the above assumption is true than in the case that it is false.

The property ($P2$) claims that the influence of systematic absences on the size of the resulting graph is limited. The influence of missing diffraction peaks due to reasons other than systematic absences is also limited, because the probability that all $|2l_1^* \pm l_2^*|^2$ and $|l_1^* \pm 2l_2^*|^2$ are missing simultaneously is small.

The above discussion supports the use of the size of the resulting graph as a sorting criterion for 2×2 metric tensors output from the algorithm in Table 1. The value of the criterion is computed by the following procedures:

(i) Enumerate combinations of four q-values q_1, q_2, q_3, q_4 of diffraction peaks satisfying $2(q_1 + q_2) = q_3 + q_4$ by the algorithm in Table 1. For every such q_1, q_2, q_3, q_4, insert the corresponding subgraph as in Fig. 1 in an array A_2. (Any subgraphs of a topograph with finite nodes and edges are implemented without difficulty by using a binary tree data structure.)

(ii) Unify subgraphs in A_2 by finding those with a common node, as in Fig. 9. For every resulting subgraph, let F be the number of diffraction peaks whose q-values are used to form the subgraph. For every entry of A_2 contained in the subgraph, define its figure of merit as F.

(iii) Remove elements with smaller figures of merit from A_2.

By procedures (i)–(iii), it is possible to reduce the number of candidate two-dimensional lattices, retaining the more plausible ones. In the program implemented by the author, the procedures (i)–(iii) finish in a moment when the number of used reflections is below 100.

Note that the above figure of merit F ignores diffraction peaks not corresponding to computed q-values. Therefore, it will be effective in finding lattices whose vectors do not correspond to all the diffraction peaks. This includes the case

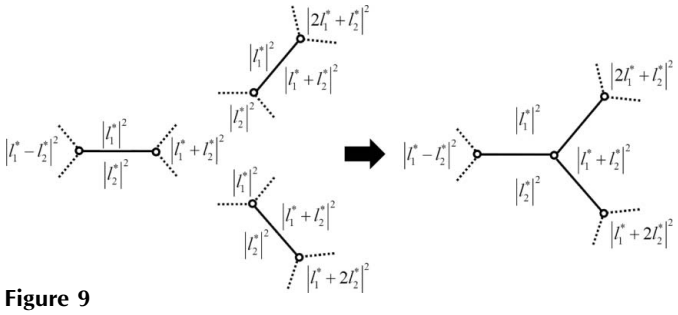

Figure 9
Extension of a subgraph of a topograph. [All three graphs on the left-hand side have a common node associated with $\{0, \pm l_1^*, \pm l_2^*, \pm(l_1^* + l_2^*)\}$. This figure illustrates how these graphs are unified.]

of zone detection, *i.e.* the search for two-dimensional sublattices of three-dimensional crystal lattices. In §5, the new figure of merit is applied for the purpose.

5. Main results on distribution rules of systematic absences

In this section, the primitive lattice of a crystal is always represented as L and distinguished from the Bravais lattice. We present a method to determine the 3×3 metric tensor of the reciprocal lattice L^* using the q-values of diffraction peaks. The method is based on the theorems introduced in this section and therefore works for any types of systematic absence. All the proof of the theorems are found in Appendix *D*.

From a powder diffraction pattern, a finite subset of the following set is extracted:

$$\Lambda^{\rm cal} := \left\{|l^*|^2 : 0 \neq l^* \in L^* \text{ does not belong to } \Gamma_{\rm ext}\right\}. \quad (16)$$

In the following, this observed finite set is denoted by $\Lambda^{\rm obs}$.

The following theorem is applicable to zone detection:

Theorem 2. Regardless of the type of systematic absence, there are infinitely many primitive sets $\{l_1^*, l_2^*\}$ of L^* such that none of l_1^*, l_2^*, $l_1^* + 2l_2^*$, $2l_1^* + l_2^*$ are contained in $\Gamma_{\rm ext}$.

As a consequence of Theorem 2, even if $\Lambda^{\rm obs}$ has missing or false q-values, $\Lambda^{\rm obs}$ normally contains $|l_1^*|^2$, $|l_2^*|^2$, $|l_1^* + 2l_2^*|^2$ and $|2l_1^* + l_2^*|^2$ for multiple primitive sets $\{l_1^*, l_2^*\}$ of L^*. The lattice vector lengths satisfy the following formula:

$$3|l_1^*|^2 + |l_1^* + 2l_2^*|^2 = 3|l_2^*|^2 + |2l_1^* + l_2^*|^2. \quad (17)$$

For the lengths $|l_1^*|^2$, $|l_2^*|^2$, $|l_1^* \pm l_2^*|^2$ satisfying Ito's equation, a completely different situation occurs for some types of systematic absence as explained in Appendix *A*.

Equation (17) corresponds to the left-hand graph in Fig. 10, which is a subgraph of the topograph defined for the two-dimensional lattice expanded by l_1^*, l_2^*.

The subgraph is composed of two edges corresponding to Ito's equation as seen in Fig. 10. In parallel with this, equation (17) is decomposed into two Ito equations by inserting the new lattice vector $l_1^* + l_2^*$:

$$2(|l_1^* + l_2^*|^2 + |l_1^*|^2) = |l_2^*|^2 + |2l_1^* + l_2^*|^2, \quad (18)$$

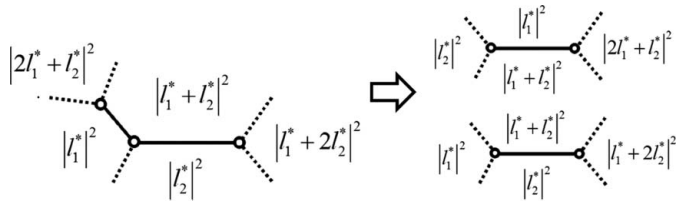

Figure 10
A subgraph of a topograph corresponding to the equation $3|l_1^*|^2 + |l_1^* + 2l_2^*|^2 = 3|l_2^*|^2 + |2l_1^* + l_2^*|^2$.

$$2(|l_1^* + l_2^*|^2 + |l_2^*|^2) = |l_1^*|^2 + |l_1^* + 2l_2^*|^2. \quad (19)$$

If $|l_1^* + l_2^*|^2$ does not correspond to any q-values in $\Lambda^{\rm obs}$, we may assume that it was not observed because of systematic absence and so on. Note that, nevertheless, $|l_1^* + l_2^*|^2$ is computed by $|l_1^* + l_2^*|^2 = (|l_2^*|^2 + |2l_1^* + l_2^*|^2)/2 - |l_1^*|^2 = (|l_1^*|^2 + |l_1^* + 2l_2^*|^2)/2 - |l_2^*|^2$ from the other vector lengths. As a result, 2×2 metric tensors of the same zone are computed from equations (18) and (19), because they correspond to edges contained in the same topograph.

There are still non-trivial problems:

($Q1$) It is possible that the equation $3q_1 + q_3 = 3q_2 + q_4$ only holds accidentally owing to, *e.g.*, false peaks caused by impurities, and L^* might not include lattice vectors l_1^*, l_2^* satisfying $q_1 = |l_1^*|^2$, $q_2 = |l_2^*|^2$, $q_3 = |l_1^* + 2l_2^*|^2$, $q_4 = |2l_1^* + l_2^*|^2$. How can we remove such mistakenly enumerated combinations?

($Q2$) How can we construct a three-dimensional solution from the obtained zones without the adverse effects of systematic absences?

These problems have not been answered in previous studies of Ito's method. We shall provide methods to resolve these problems.

We may expect ($Q1$) to be resolved by the same procedures (i)–(iii) in §4. It is only necessary to verify that the influence of systematic absences is also limited in the case of space groups. This is ascertained by the following theorem:

Theorem 3. Regardless of the type of systematic absence, there are infinitely many primitive sets $\{l_1^*, l_2^*\}$ of L^* such that $ml_1^* + (m-1)l_2^*$ does not belong to $\Gamma_{\rm ext}$ for any integer m. Furthermore, there exist infinitely many two-dimensional sublattices L_2^* of L^* such that L_2^* is expanded by a primitive set $\{l_1^*, l_2^*\}$ of L^* satisfying this property.

The lattice vectors $ml_1^* + (m-1)l_2^*$ ($m \in \mathbb{Z}$) satisfy equation (17) as follows:

$$\begin{aligned} &3|ml_1^* + (m-1)l_2^*|^2 + |(m+2)l_1^* + (m+1)l_2^*|^2 \\ &\quad = 3|(m+1)l_1^* + ml_2^*|^2 + |(m-1)l_1^* + (m-2)l_2^*|^2. \end{aligned} \quad (20)$$

Hence Theorem 2 is obtained as a corollary of Theorem 3. By connecting the subgraphs corresponding to equation (20) for each m, a chain of infinite length as in Fig. 11 is obtained. Theorem 3 indicates that a large subgraph is formed by unifying the subgraphs associated with q-values of $\Lambda^{\rm obs}$. (However, the size of the formed graph is rather limited because the number of q-values in $\Lambda^{\rm obs}$ should not exceed 100

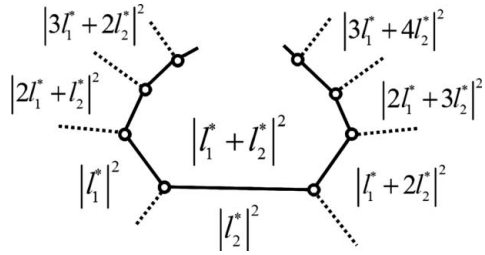

Figure 11
A connected chain contained in a topograph.

if observation errors included in large q-values are considered properly.)

($Q2$) is resolved by the following theorem:

Theorem 4. Regardless of the type of systematic absence, there are infinitely many bases $\langle l_1^*, l_2^*, l_3^* \rangle$ of L^* such that the following hold:

(a) $\pm l_1^* + l_2^* + l_3^*$ do not belong to $\Gamma_{\rm ext}$.

(b) For both $i = 2, 3, ml_1^* + (m-1)(-l_1^* + l_i^*)$ do not belong to $\Gamma_{\rm ext}$ for any integer m, or $ml_i^* + (m-1)(l_1^* - l_i^*)$ do not belong to $\Gamma_{\rm ext}$ for any integer $m \geq 0$.

That is, none of the underlined lattice vectors in Fig. 12 belong to $\Gamma_{\rm ext}$.

Consequently, candidate solutions for the 3×3 metric tensor of L^* are enumerated by the following procedure, which is almost identical to the algorithm adopted in the powder auto-indexing program *Conograph*. (In the following procedure, the assertion that $-l_1^* + l_2^* + l_3^* \notin \Gamma_{\rm ext}$ is not used, for simplicity.)

(i) Enumerate combinations of four q-values q_1, q_2, q_3, q_4 in $\Lambda^{\rm obs}$ satisfying $3q_1 + q_3 = 3q_2 + q_4$. From each combination, obtain two sets of q-values satisfying Ito's equation by the method described above. Insert every set in an array A_2.

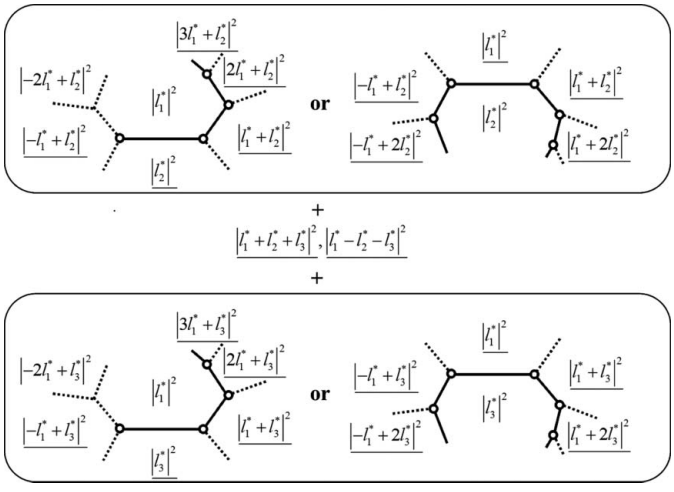

Figure 12
A set of q-values that can be used for enumeration of three-dimensional lattices. (In the process of determining the 3×3 metric tensors of the lattice, it may be assumed that the lengths of all the underlined lattice vectors are included in $\Lambda^{\rm obs}$.)

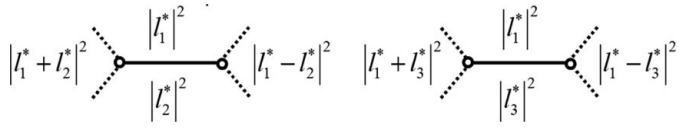

Figure 13
Two edges associated commonly with l_1^*. [When two Ito equations $2(q_1 + q_2) = q_3 + q_4$ and $2(r_1 + r_2) = r_3 + r_4$ are provided, we judge whether $q_1 = r_1$ holds by the following procedure: first, if q_1 and r_1 refer to the same q-values in $\Lambda^{\rm obs}$, it may be supposed that $q_1 = r_1$. If q_1, r_1 are not in $\Lambda^{\rm obs}$, they are q-values obtained by decomposing equation (17) into two Ito equations and computed by $q_1 := (q_3 + q_4)/2 - q_2$ and $r_1 := (r_3 + r_4)/2 - r_2$. Thus q_1 and r_1 may be considered to be equal as long as $(q_3 + q_4)/2 - q_2$ and $(r_3 + r_4)/2 - r_2$ coincide under consideration of their observation errors.]

(ii) Compute the figure of merit for all entries of A_2 using the method described in §4. Remove entries with smaller figures of merit from A_2.

(iii) For any q-value q_0 in $\Lambda^{\rm obs}$ and two entries of A_2 corresponding to Ito's equation 2 $(|l_1^*|^2 + |l_i^*|^2) = |l_1^* + l_i^*|^2 + |l_1^* + l_i^*|^2$ $(i = 2, 3)$ as in Fig. 13, assume that $q_0 = |l_1^* + l_2^* + l_3^*|^2$ holds. The 3×3 metric tensor $(l_i^* \cdot l_j^*)_{1 \leq i,j \leq 3}$ is computed as follows:

$$\begin{pmatrix} |l_1^*|^2 & \frac{|l_1^*+l_2^*|^2-|l_1^*|^2-|l_2^*|^2}{2} & \frac{|l_1^*+l_3^*|^2-|l_1^*|^2-|l_3^*|^2}{2} \\ \frac{|l_1^*+l_2^*|^2-|l_1^*|^2-|l_2^*|^2}{2} & |l_2^*|^2 & \frac{|l_1^*|^2-|l_1^*+l_2^*|^2-|l_1^*+l_3^*|^2+q_0}{2} \\ \frac{|l_1^*+l_3^*|^2-|l_1^*|^2-|l_3^*|^2}{2} & \frac{|l_1^*|^2-|l_1^*+l_2^*|^2-|l_1^*+l_3^*|^2+q_0}{2} & |l_3^*|^2 \end{pmatrix}. \tag{21}$$

Insert the metric tensor in an array A_3, if it is positive definite.

The use of the figure of merit in (ii) is justified by property (b) of Theorem 4. The lengths used in (iii) including $|\pm l_1^* + l_2^* + l_3^*|^2$ may be considered to be associated with every circuit of length 6 as in Fig. 6.

In this paper, we did not define a sorting criterion for 3×3 metric tensors. For two-dimensional lattices, we have explained that a large graph associated with observed q-values is formed by connecting subgraphs corresponding to Ito's equation. For three-dimensional lattices, a rather large subgraph seems to be formed by connecting circuits of length 6, although we have not investigated this sufficiently. Such a criterion is expected to be effective for powder diffraction patterns including false peaks due to impurities.

6. Conclusion

We have introduced unknown general properties of systematic absences. They are given as distribution rules of extinct Miller indices on a topograph. A new powder auto-indexing algorithm, which works for any Bravais lattices, space groups and systematic absences, was proposed based on these rules. The algorithm was implemented in the powder auto-indexing software *Conograph*. Detailed information about other advantages, parameter settings and results of *Conograph* will be provided in our subsequent paper.

7. Related literature

Appendix *A* also mentions the equations suggested by de Wolff (1957), in addition to Ito's equation. A theorem in Milnor (1971) was used to obtain the statements about the structure of topographs for three-dimensional lattices (see Appendix *C*). The space-group library of the Z-Rietveld code (Oishi-Tomiyasu *et al.*, 2012) was used to find and prove the distribution rules given here.

I would like to thank Dr S. Torii, Dr J. Zhang, Dr M. Ping, Professor M. Yonemura and Professor T. Kamiyama of KEK; Professor A. Hoshikawa and Professor T. Ishigaki of Ibaraki University; and Dr K. Fujii, Professor H. Uekusa and Professor T. Ozeki of the Tokyo Institute of Technology for their valuable comments and for offering test data. I would also like to express my gratitude to Professor T. Oda of the University of Tokyo for his daily encouragement, to Visible Information Inc. for their cooperation in implementing the *Conograph* GUI, and to Professor E. Hitzer of the International Christian University for proposing the impressive name '*Conograph*'. This research was partly supported by a Grant-in-Aid for Young Scientists (B) (No. 22740077) and the Ibaraki Prefecture (J-PARC-23D06).

References

Conway, J. H. (1997). *The Sensual (Quadratic) Form*. Carus Mathematical Monographs 26. Washington: Mathematical Association of America.
Delaunay, B. (1933). *Z. Kristallogr.* **84**, 109–149.
Hahn, Th. (1983). Editor. *International Tables for Crystallography*, Vol. A. Dordrecht: Kluwer.
Ito, T. (1949). *Nature (London)*, **164**, 755–756.
Milnor, J. (1971). *Introduction to Algebraic K-theory*. *Annals of Mathematical Studies*, edited by P. A. Griffiths, J. N. Mather & E. M. Stein. Princeton University Press.
Oishi-Tomiyasu, R. (2012). *Acta Cryst.* A**68**, 525–535.
Oishi-Tomiyasu, R., Yonemura, M., Ishigaki, T., Hoshikawa, A., Mori, K., Morishima, T., Torii, S. & Kamiyama, T. (2009). *Z. Kristallogr. (Suppl.)*, **30**, 15–20.
Oishi-Tomiyasu, R., Yonemura, M., Morishima, T., Hoshikawa, A., Torii, S., Ishigaki, T. & Kamiyama, T. (2012). *J. Appl. Cryst.* **45**, 299–308.
Ryškov, S. S. (1976). *J. Math. Sci.* **6**, 651–671.
Selling, E. (1874). *J. Reine Angew. Math.* **77**, 143–229.
Visser, J. W. (1969). *J. Appl. Cryst.* **2**, 89–95.
Wolff, P. M. de (1957). *Acta Cryst.* **10**, 590–595.
Wolff, P. M. de (1958). *Acta Cryst.* **11**, 664–665.